Geophys. J. Int. (2004) **157,** 1146–1151 doi: 10.1111/j.1365-246X.2004.02330.x

FAST TRACK PAPER

Constraints on density and shear velocity contrasts at the inner core boundary

Aimin Cao and Barbara Romanowicz
Seismological Laboratory, University of California, Berkeley, California, USA. E-mail: barbara@seismo.berkeley.edu

Accepted 2004 March 20. Received 2004 March 20; in original form 2003 September 26

GJI Seismology

SUMMARY

The density jump ($\Delta\rho_{\rm ICB}$) at the inner core boundary (ICB) is an important constraint on the dynamics and history of the Earth's core. Two types of seismological data sensitive to $\Delta\rho_{\rm ICB}$ have been studied since the 1970s: free oscillation eigenfrequencies and the amplitudes of core reflected phases (*PKiKP*/*PcP*). The preliminary reference earth model (PREM) of Dziewonski & Anderson, based largely on normal mode data, has a relatively low value of $\Delta\rho_{\rm ICB} = 0.60$ g cm^{-3}, whereas most studies based on *PKiKP*/*PcP* amplitude ratios find significantly larger values, sometimes in excess of 1.0 g cm^{-3}. It has been argued that, because *PKiKP* is rarely observed in the distance range considered (10–70°), the latter type of measurement provides only upper bounds on $\Delta\rho_{\rm ICB}$. We have analysed 10 yr of high-quality global broad-band data accumulated since the work of Shearer & Masters. We systematically analysed over 4500 seismograms from intermediate/deep events (depth >70 km) and nuclear explosions in the distance range 10–70°. The data were filtered in the bandpass 0.7–3 Hz. We performed rigorous data selection and identified five pairs of very clear (quality A), and 15 possible (quality A$^-$) *PKiKP* and *PcP* arrivals. In addition, 58 records showed no *PKiKP* but a clear *PcP*. Together, we obtain a much less dispersed data set than previously available, with the quality A data at the lower end of the ensemble of amplitude ratios versus distance. We combine our high-quality measurements with two measurements from the literature that fall within our rigorous selection criteria and obtain estimates of $\Delta\rho_{\rm ICB}$ in the range 0.6–0.9 g cm^{-3} and $\Delta\beta_{\rm ICB}$ in the range 2–3 km s^{-1}. Our estimate of $\Delta\rho_{\rm ICB}$ is in agreement with a recent re-evaluation of normal mode data, thus reconciling results from body wave and mode studies and providing a tighter constraint on $\Delta\rho_{\rm ICB}$ for geodynamicists. Our study also provides evidence for a shear velocity gradient at the top of the inner core.

Key words: density contrast, ICB, inner core, *PKiKP*/*PcP* amplitude ratio, *S*-velocity contrast.

1 INTRODUCTION

The density $\Delta\rho_{\rm ICB}$ and shear velocity $\Delta\beta_{\rm ICB}$ contrasts at the inner core boundary (ICB), estimated using seismological methods, are important constraints for the understanding of the character of the Earth's geodynamo and the evolution of the inner core (e.g. Hewitt *et al.* 1975; Gubbins 1977; Buffett *et al.* 1996; Stacey & Stacey 1999).

So far, three distinct approaches have been used to constrain the density and shear velocity contrasts at the ICB, but the resulting estimates vary significantly. The first method uses data for normal modes which are sensitive to the structure of the inner core (Dziewonski & Gilbert 1971; Gilbert *et al.* 1973; Gilbert & Dziewonski 1975; Masters 1979). The preliminary reference earth model (PREM) of Dziewonski & Anderson (1981), which incorporates constraints from normal mode data, has $\Delta\rho_{\rm ICB} = 0.60$ g cm^{-3} and $\Delta\beta_{\rm ICB} = 3.5$ km s^{-1}.

The second method uses body wave amplitude and waveform modelling of *PKP* and *PKiKP*. This technique has resulted in estimates of $\Delta\rho_{\rm ICB} \sim 0$–1.2 g cm^{-3} (Häge 1983) and $\Delta\beta_{\rm ICB}$ ranging from ~0 km s^{-1} (Choy & Cormier 1983) to 2.5–3.0 km s^{-1} (Häge 1983) or 2–4 km s^{-1} (Cummins & Johnson 1988).

The third method is based on measurements of *PKiKP*/*PcP* amplitude ratios in the distance range 10–70°. The first convincing observation of *PKiKP* in this distance range was reported by Engdahl *et al.* (1970) and was based on stacking of LASA array data. Bolt & Qamar (1970) first proposed the amplitude ratio technique and estimated a maximum density jump of 1.8 g cm^{-3} at the ICB. Souriau & Souriau (1989) further constrained the density jump to be in the range of 1.35–1.6 g cm^{-3} based on array data. Finally, Shearer & Masters (1990) estimated maximum bounds on *PKiKP*/*PcP* ratios and obtained $\Delta\rho_{\rm ICB} < 1.0$ g cm^{-3} and $\Delta\beta_{\rm ICB} >$ 2.5 km s^{-1}.

Compared with the results derived from normal modes, the constraint on the density contrast from body waves is considered to be much less robust, as it is based on few reliable measurements, and most recently a set of rather scattered 'upper bound' data (Shearer & Masters 1990). Indeed, *PKiKP* is such a weak phase in the distance range from 10–70° that it is rarely observed, and even more rarely so without stacking. Shearer & Masters (1990) systematically searched for *PKiKP* arrivals in over 4900 Global Digital Seismic Network (GDSN) vertical component seismograms. They found only two seismograms with both clear *PKiKP* and *PcP* arrivals. Both Souriau & Souriau (1989) and Shearer & Masters (1990) used 'non-observations' of *PKiKP* as upper bounds on the observed amplitude of this phase, leading to upper bounds on the corresponding *PKiKP*/*PcP* amplitude ratios.

At present, geodynamo simulations usually refer to the density contrast derived from normal mode data. Nevertheless, a recent geodynamo study (Stacey & Stacey 1999) explicitly pointed out that the inner core would not have existed 2 billion years ago if the density contrast at the ICB was as low as inferred from current seismological models. This is obviously against the palaeomagnetic evidence, which shows that the Earth has sustained a magnetic field for at least 3 billion years (McElhinny & Senanayake 1980).

In this study, we take advantage of the accumulation of large quantities of high-quality global broad-band seismic data in the last 15 yr to revisit the question of estimating the density and shear velocity contrasts at the ICB using *PKiKP*/*PcP* amplitude ratios.

2 DATA, METHOD AND RESULTS

All of the broad-band vertical component data for deeper (≥70 km) natural earthquakes and nuclear explosions in the distance range 10–70°, for the time span 1990–1999, were systematically downloaded from the IRIS Data Management Center (DMC), to search for simultaneous observations of *PKiKP* and *PcP*. The ray paths of these phases for a given source–station pair are shown in Fig. 1. The seismograms were filtered in the bandpass 0.7–3 Hz (the dominant frequency of *PKiKP* is typically ∼1 Hz). We used relocated origin time and hypocentral parameters from the catalogue of

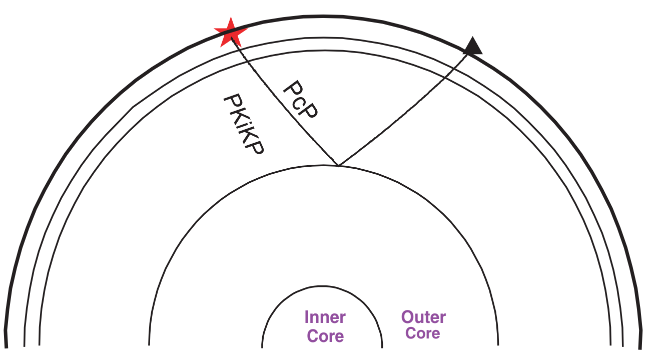

Figure 1. Ray paths of *PKiKP* (reflected *P* wave from the ICB) and *PcP* (reflected *P* wave from the CMB). The star denotes an assumed source and the triangle denotes a seismological station.

Engdahl *et al.* (1998), recently extended to include the year 1999. We then marked the seismograms with the theoretical arrival times of 11 phases (*PcP*, *PKiKP* as well as *P*, *pP*, *sP*, *PP*, *PPP*, *S*, *sS*, *SS* and *ScS*) computed with respect to model AK135 (Kennett *et al.* 1995), and corrected for ellipticity (Dziewonski & Gilbert 1976). Those nine phases are the most likely ones to interfere with our target *PcP* and PKiKP phases. Finally only those seismograms were kept whose background noise before the direct *P* wave was significantly less than the average amplitude level in the vicinity of the theoretical *PKiKP* arrival.

We divided the resulting 79 seismograms (out of an initial collection of more than 4500) into three categories (A, A^- and B), according to the following criteria. Quality A data exhibit very clear *PKiKP* and *PcP* phases within 5 s of their expected theoretical arrivals, there is no other theoretical arrival 15 s preceding or following the identified *PKiKP* or *PcP* phases (unless the potential interfering arrival can be verified from a nodal plane inspection), and the average peak-to-peak noise-to-signal ratio is less than 40 per cent. Quality A^- includes seismograms with clear *PKiKP* and *PcP* phases within 5 s of their theoretical arrivals, there is no other theoretical arrival 15 s preceding or following the identified *PKiKP* or *PcP*, but the average peak-to-peak noise-to-signal ratio is larger than 40 per cent. Finally, in quality B, we collected seismograms with no observable *PKiKP* phase within 5 s of its theoretical arrival, but there is also no other predicted arrival 50 s preceding and 10 s following the theoretical *PKiKP* arrival, and the *PcP* phase is very clear and within 5 s of its predicted arrival.

Based on the above criteria, we collected 5, 15 and 59 quality A, A^- and B data, respectively. All of our quality A data are shown in Fig. 2. We measured peak-to-peak amplitudes of the identified *PKiKP* and *PcP* phases and computed *PKiKP*/*PcP* amplitude ratios for quality A and A^- data. For quality B data, the maximum peak-to-peak amplitude 5 s around the *PKiKP* theoretical arrival was used as an upper limit for the *PKiKP* amplitude (e.g. Shearer & Masters 1990). In the epicentral distance range considered, for quality A data, the difference in take-off angles between *PKiKP* and *PcP* is small (approximately from 2.3° to 11.9°) and the two rays are close to the maxima of the radiation lobes, as we have verified (Fig. 2). Therefore, the effect of the radiation pattern at the source is neglected (e.g. Souriau & Souriau 1989).

Additionally, we also applied our selection criteria to re-examine available seismograms from the literature. Shearer & Masters (1990) identified only two seismograms with clear simultaneous *PKiKP* and *PcP* observations. The theoretical *SS* arrival is only 1.97 s in front of the theoretical *PKiKP* arrival for the first seismogram. For their second seismogram, a theoretical *SS* arrival is 13.38 s in front of the theoretical *PKiKP* arrival with reference to model AK135. Hence it is possible that the discrepancy in the corresponding *PKiKP*/*PcP* amplitude ratios (almost a factor of 3) is due to interference with *SS* in the first example, even though the corresponding epicentral distances are almost the same (39.8° and 39.2° respectively). We included the second of these two measurements, which, according to our criteria, is much more reliable, in our quality A data set. We also included one stacking measurement (0.032, $\Delta = 51.4°$) (Schweitzer 1992), which has recently been remeasured (0.038–0.048) by the author himself (Schweitzer, personal communication, 2003).

We then compared our *PKiKP*/*PcP* amplitude ratio measurements with theoretical predictions using several reference models: PREM (Dziewonski & Anderson 1981), PREM2 (Song & Helmberger 1995), IASP91 (Kennett & Engdahl 1991) and AK135 (Kennett *et al.* 1995). Models differ by the velocity contrasts and

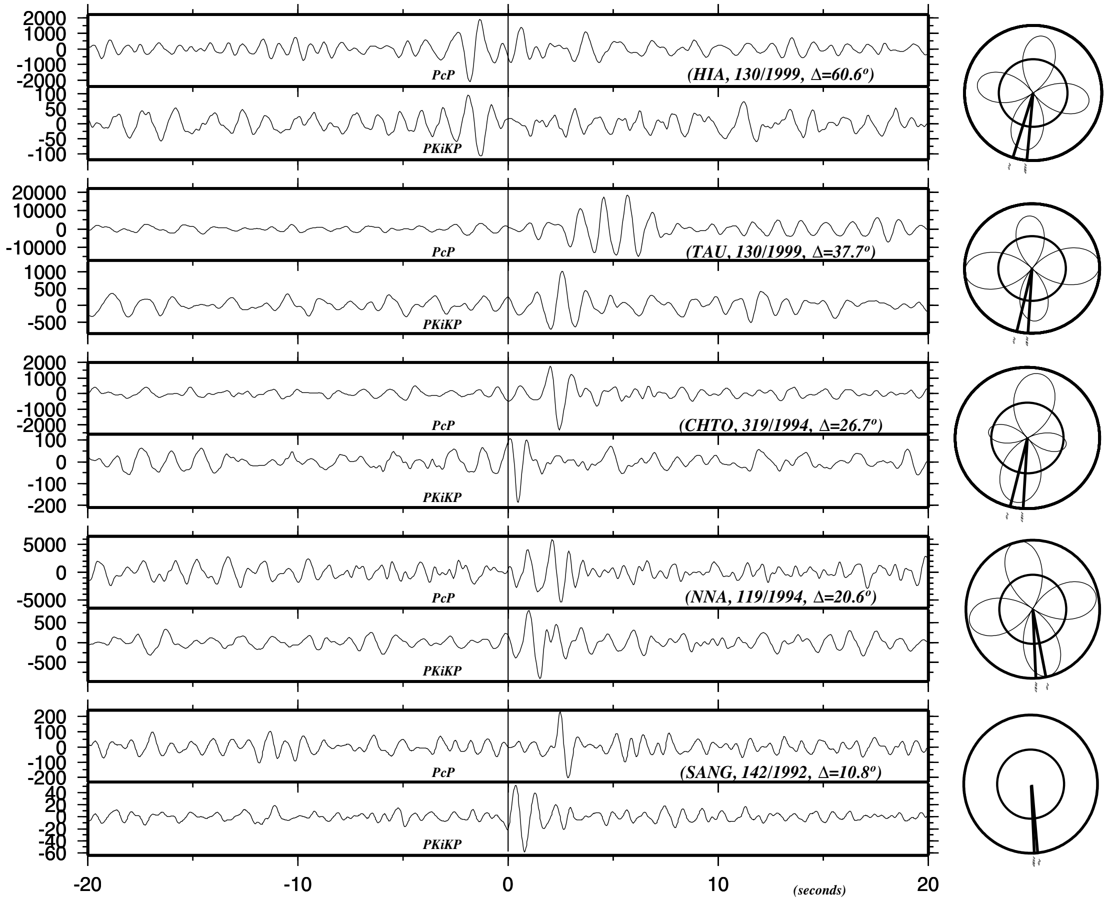

Figure 2. Quality A observations with very clear *PKiKP* and *PcP* phases. Dashed lines are the theoretical arrival times referring to the AK135 seismic model, taking into account ellipticity corrections. From top to bottom, the observed *PKiKP*/*PcP* amplitude ratios are 0.052, 0.052, 0.071, 0.151 and 0.250 respectively. To the right of each pair of traces are the corresponding *P*-wave radiation patterns derived from the Harvard CMT moment tensors. From top to bottom the differential take-off angles between *PKiKP* and *PcP* are approximately 11.9°, 9.6°, 10.0°, 8.6° and 2.3° respectively. The last observation (SANG) corresponds to a nuclear explosion event.

Table 1. Comparison of seismic contrasts at ICB and CMB in the four models. Units of velocity and density contrasts are km s^{-1} and g cm^{-3} respectively.

Models	$\Delta\alpha_{\rm ICB}$	$\Delta\alpha_{\rm CMB}$	$\Delta\beta_{\rm ICB}$	$\Delta\beta_{\rm CMB}$	$\Delta\rho_{\rm ICB}$	$\Delta\rho_{\rm CMB}$
PREM	0.67	5.65	3.50	7.26	0.60	4.34
PREM2	0.78	5.45	3.50	7.26	0.60	4.34
IASP91	0.83	5.68	3.44	7.30	0.56	4.36
AK135	0.75	5.66	3.50	7.28	0.56	4.36

density contrasts at the ICB and core–mantle boundary (CMB) (Table 1).

In order to obtain the theoretical *PKiKP*/*PcP* amplitude ratio, we calculated transmission and reflection coefficients at various seismic discontinuities as well as ratios of *PKiKP* and *PcP* geometrical spreading factors, which may be readily expressed as functions of ray parameters and their corresponding derivatives (Bolt & Qamar 1970). As for the attenuation factor, we neglected its effect on the predicted ratios in the mantle due to the arguably close ray paths of *PKiKP*/*PcP* there, and we assumed that the quality factor in the outer core is infinite because there is no significant change when using a realistic quality factor (≥10 000) (Cormier & Richards 1976). As previous authors, we also neglected finite frequency effects as these are probably within the uncertainties of other factors such as the earth models used, in particular a possible topography of the CMB. When we explored different models, the computed geometrical spreading factors were very close but reflection coefficients varied significantly. For each of the models, we searched for the best variance reduction in the parameter space ($\Delta\rho_{\rm ICB}$, $\Delta\beta_{\rm ICB}$). We note that the set of quality A measurements spans the entire epicentral distance range considered (Fig. 3), thus providing relatively tight fits on the resulting ICB parameters: $\Delta\beta_{\rm ICB}$ is constrained at large distances ($\Delta > 50°$) whereas $\Delta\rho_{\rm ICB}$ is constrained by data at shorter distances. The best-fitting density contrasts at the ICB vary somewhat from one model to the other, as illustrated in Fig. 4: from ∼0.6 g cm^{-3} (IASP91) to ∼0.9 g cm^{-3} (PREM2). On the other hand, the range of the best-fitting shear velocity contrasts is somewhat tighter: from ∼2.4 km s^{-1} to ∼2.6 km s^{-1}. In fact, because the shear velocity and density contrasts at the CMB are very consistent in each model, the uncertainty in $\Delta\rho_{\rm ICB}$ and $\Delta\beta_{\rm ICB}$ stems mostly from the difference in $\Delta\alpha_{\rm ICB}$ and $\Delta\alpha_{\rm CMB}$ for the different models. In particular, the results for IASP91 show the lowest $\Delta\rho_{\rm ICB}$ because its $\Delta\alpha_{\rm ICB}$ is significantly larger (>6 per cent) than for the other models.

3 DISCUSSION

In our study, we have identified seven definite *PKiKP* arrivals and 15 probable ones, but compared with the huge initial data pool the percentage of observations is still quite small. It has been argued

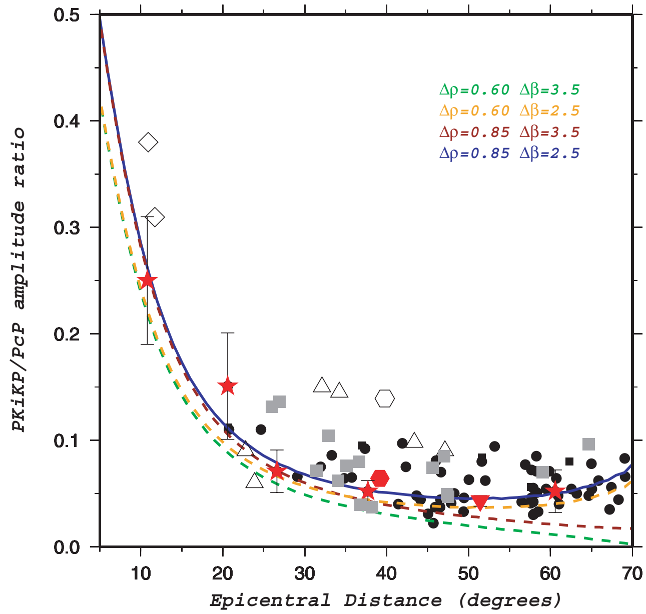

Figure 3. Measurements of *PKiKP*/*PcP* amplitude ratios. The red stars denote the quality A data, and their error bars are derived from the fractional ratios of the average peak-to-peak amplitudes of background noise to the peak-to-peak amplitude of the identified phase arrivals; the red hexagon is Shearer & Masters' (1990) second measurement with clear *PKiKP*; the inverted red triangle is a stacking measurement (Schweitzer 1992) which has been remeasured by the author himself recently; the grey squares denote the quality A$^-$ data; the black dots are the quality B data. The curves are the theoretical *PKiKP*/*PcP* amplitude ratios calculated with respect to the PREM model. For the dashed green curve $\Delta\rho_{\rm ICB} = 0.60$ g cm^{-3} and $\Delta\beta_{\rm ICB} = 3.5$ km s^{-1} (original values in the PREM model); for the dashed orange curve $\Delta\rho_{\rm ICB} = 0.60$ g cm^{-3} and $\Delta\beta_{\rm ICB} = 2.5$ km s^{-1}; for the dashed red curve $\Delta\rho_{\rm ICB} = 0.85$ g cm^{-3} and $\Delta\beta_{\rm ICB} = 3.5$ km s^{-1}; and for the solid blue curve $\Delta\rho_{\rm ICB} = 0.85$ g cm^{-3} and $\Delta\beta_{\rm ICB} = 2.5$ km s^{-1} (our best-fitting values using the PREM model). The open symbols are other data from previous studies, which were not used in our analysis (triangles, Souriau & Souriau (1989); hexagon, Shearer & Masters (1990); diamonds, Engdahl *et al.* (1970) and Bolt & Qamar (1970)).

that *PKiKP* is observable only when it is anomalously large, probably due to focusing from heterogeneities within the Earth, and even the *PKiKP*/*PcP* data measured from the identified *PKiKP* arrivals represent only upper limits for this ratio (Souriau & Souriau 1989; Shearer & Masters 1990). However, when we compare our quality A, A$^-$ and B measurements (Fig. 3), we note the following: (1) the data are overall much less scattered than in previous studies and (2) the quality A measurements generally fall near the lower bound of all our measurements, including those found in the literature and corresponding to explicit reports of *PKiKP* observations. We thus believe that although the *PKiKP* arrival is generally weak, our quality A observations are not significantly biased either by interfering phases (we ruled those out) or focusing effects, and that they simply correspond to favourable geometry with respect to the maximum in *P* radiation pattern, as we have checked. On the other hand, some of our A$^-$ measurements plot above the best-fitting theoretical curves computed using only the quality A data, which indicates that, for these measurements, there may be some constructive interference between noise and *PKiKP*. We did not use these data in computing the optimal ICB parameters, but we find that they are compatible with the resulting predictions, as are our quality *B* data (Fig. 3).

On the other hand, we did not include other data from the literature for which seismograms were not available for verification (we show them as open symbols in Fig. 3.). In particular, several previous measurements used stacking of traces (e.g. Bolt & Qamar 1970; Souriau & Souriau 1989). The stacking technique is very effective in extracting the weak seismic signal, but it seems difficult to keep the amplitudes of *PKiKP* and *PcP* arrivals from being distorted in the summation (especially when using a non-linear stacking process).

The density contrast inferred at the ICB depends on the reference seismic models (Fig. 4). The main reason is that the reflection coefficients of *PcP* at the CMB and *PKiKP* at the ICB also depend on the corresponding *P*-wave velocity contrasts. In general, the larger $\Delta\alpha_{\rm ICB}$, the lower $\Delta\rho_{\rm ICB}$, for a fixed $\Delta\alpha_{\rm CMB}$; and the larger $\Delta\alpha_{\rm CMB}$, the lower $\Delta\rho_{\rm ICB}$, for a fixed $\Delta\alpha_{\rm ICB}$. Further refinement of $\Delta\rho_{\rm ICB}$ will depend on the improvement of our knowledge of *P*-wave velocity structure at both ICB and CMB. In the four reference seismic models, PREM (Dziewonski & Anderson 1981) and IASP91 (Kennett & Engdahl 1991) are based on absolute traveltimes from the International Seismological Center (ISC) and free oscillation eigenfrequencies. PREM2 (Song & Helmberger 1995) is modified from PREM by fitting *PKP* differential traveltimes, amplitude ratios and waveforms, but shear velocity and density structure in PREM are left untouched. AK135 (Kennett *et al.* 1995) is updated from IASP91 by the authors themselves taking additional account of *PKP* differential traveltimes and event relocations. The differences in velocity between AK135 and IASP91 are generally very small except for the reduced velocity gradients at the ICB in AK135. From our experience (Tkalčić *et al.* 2002) AK135 gives better fits to *PKP* traveltime data than PREM and IASP91. We are therefore inclined to favour the bounds obtained from AK135. The main difference between PREM and IASP91 is in the $\Delta\alpha_{\rm ICB}$; and the main difference between PREM2 and AK135 is in $\Delta\alpha_{\rm CMB}$ (Table 1). We note from Figs 3 and 4 that the PREM $\Delta\rho_{\rm ICB} = 0.6$ g cm^{-3} is clearly a minimum value compatible with the data, and that $\Delta\rho \approx 0.85$ g cm^{-3} is optimal.

Compared with the constraint on $\Delta\rho_{\rm ICB}$, the constraint on $\Delta\beta_{\rm ICB}$ (2–3 km s^{-1}) is almost independent of the seismic models. While compatible with the results of other body wave studies, this well-constrained value is significantly lower than the average shear velocity contrast ($\sim$3.5 km s^{-1}) estimated from normal mode data. It is constrained by the trend in *PKiKP*/*PcP* amplitude ratios at distances $\Delta > 50°$ (Fig. 3). This may provide further evidence for the existence of a shear velocity gradient at the top of the inner core (e.g. Choy & Cormier 1983; Häge 1983; Cummins & Johnson 1988). Indeed, normal mode data provide an estimate averaged over depths of tens of kilometres, whereas the reflected wave data considered here provide a much more local estimate.

In the quality A observations, which we used to constrain density and shear velocity contrasts at the ICB, all of the corresponding focal depths of the natural events are deeper than 100 km. The usually shorter source–time functions than those of shallow (<70 km) events (with equivalent magnitudes) enhance the sharpness and signal-to-noise ratio of the phase arrivals. This beneficial feature may significantly help us to uniquely identify the weak *PKiKP* arrivals. Although our strict selection criteria have limited the global coverage of our observations, the quality A data span a wide geographical distribution (Fig. 5). The *PKiKP* (*PcP*) bouncing points at the ICB (also CMB) are located beneath the western Pacific Ocean, Australia, southeastern Asia, central Asia, eastern Europe and South America.

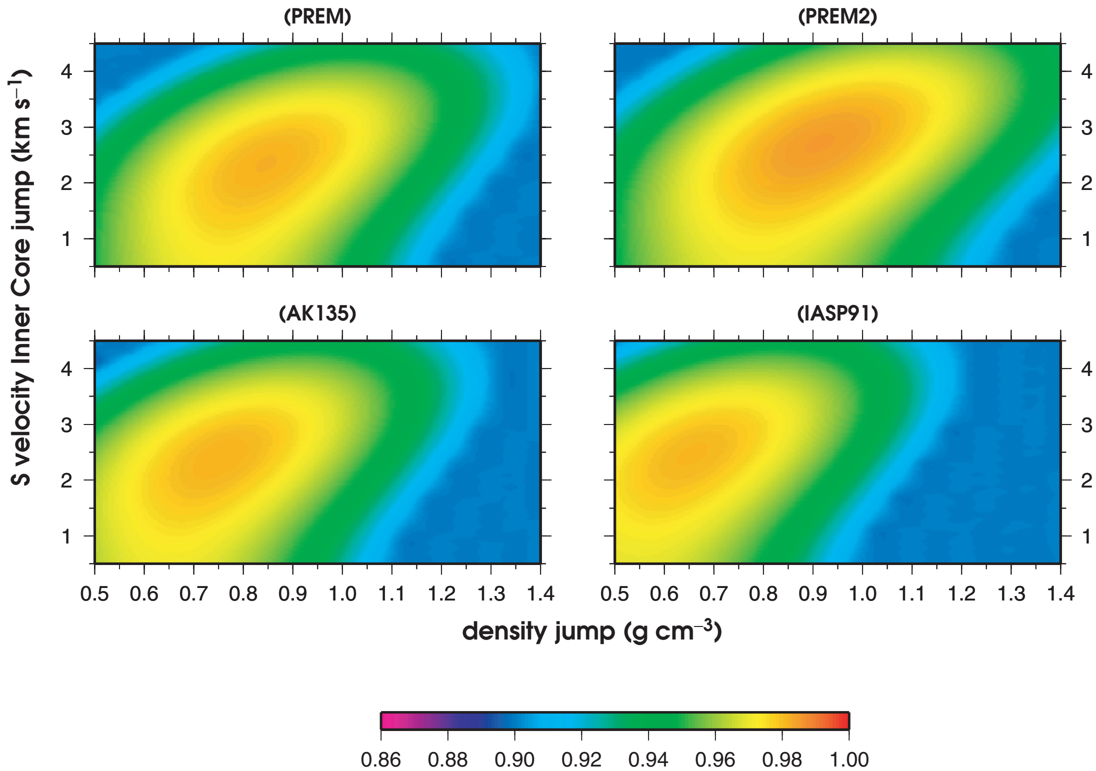

Figure 4. Variance reduction with respect to PREM (Dziewonski & Anderson 1981), PREM2 (Song & Helmberger 1995), IASP91 (Kennett & Engdahl 1991) and AK135 (Kennett *et al.* 1995). The best-fitting $\Delta\rho_{\mathrm{ICB}}$ and $\Delta\beta_{\mathrm{ICB}}$ are $\sim$0.85 g cm^{-3} and $\sim$2.5 km s^{-1}, $\sim$0.91 g cm^{-3} and $\sim$2.6 km s^{-1}, $\sim$0.65 g cm^{-3} and $\sim$2.5 km s^{-1} and $\sim$0.75 g cm^{-3} and $\sim$2.4 km s^{-1} respectively.

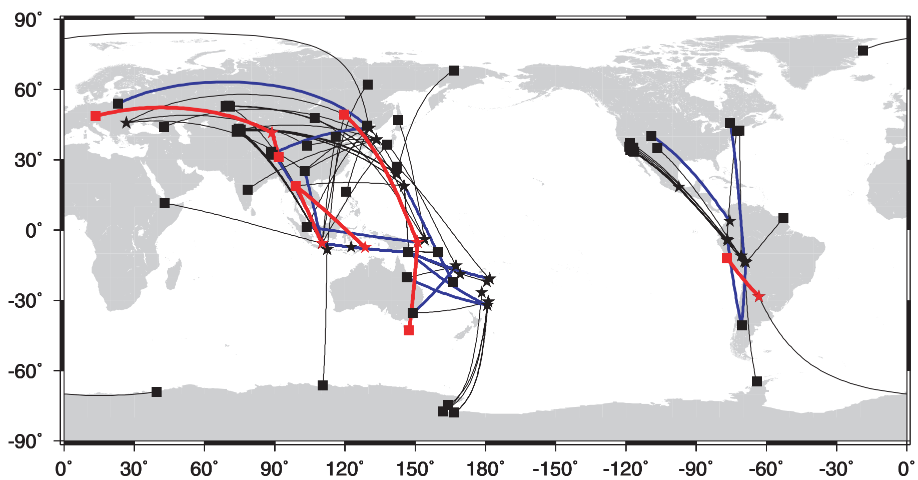

Figure 5. Geographical distribution of *PKiKP* and *PcP* ray paths. The red, blue and black lines correspond to quality A, A$^-$ and B subsets of data respectively. The stars denote the events and the squares denote the stations.

4 CONCLUSIONS

We have obtained a set of high-quality *PKiKP* and *PcP* observations in the distance range 10–70° that provide tighter constraints on the density and shear velocity contrasts at the ICB. The identification of arguably unbiased *PKiKP* and *PcP* arrivals greatly improves the body wave constraints on the density and shear velocity contrasts at the ICB. Our preferred value for $\Delta\rho_{\mathrm{ICB}}$ is $\sim$0.85 g cm^{-3}, with some uncertainties remaining, primarily due to uncertainties in the *P*-wave velocity contrast at the ICB. Our estimates are compatible with a recent re-evaluation (0.64–1.0 g cm^{-3}) of normal mode data (Masters & Gubbins 2003), thus reconciling previously incompatible results from normal mode and body wave measurements. On the other hand, the shear velocity contrast at the ICB is somewhat lower than the average shear velocity in the inner core as obtained from normal mode data. Our study thus provides evidence for (1) a larger density contrast at the ICB than generally assumed in dynamo studies and (2) the existence of a gradient of structure at the top of the inner core. The former is of significance for studies of the geodynamo, whose energy is proportional to the assumed density contrast (Stacey & Stacey 1999). The inferred gradient may also provide constraints on the cooling and solidifying processes in the inner core and may be of significance in studies of the geodynamo, as well as of the chemical and physical evolution of the inner core (e.g. Gubbins 1977; Loper 1978, 1991; Gubbins *et al.* 1979).

ACKNOWLEDGMENTS

This study benefited from enlightening discussion with A. Souriau, P. Shearer and J. Schweitzer. We thank G. Masters for a preprint of his paper with D. Gubbins. We are grateful to the IRIS Data Management Center (DMC) for making waveform data readily available, and to the network or station operators who contributed data to the DMC. This material is based upon work partially supported by the National Science Foundation under grant no EAR-0308750, and this is Berkeley Seismological Laboratory contribution #04-01.

REFERENCES

Bolt, B.A. & Qamar, A., 1970. Upper bound to the density jump at the boundary of the Earth's inner core, *Nature,* **228,** 148–150.

Buffett, B.A., Huppert, H.E., Lister, J.R. & Woods, A.W., 1996. On the thermal evolution of the Earth's core, *J. geophys. Res.,* **101,** 7989–8006.

Choy, G.L. & Cormier, V.F., 1983. The structure of the inner core inferred from short-period and broadband GDSN data, *Geophys. J. R. astr. Soc.,* 21–29.

Cormier, V.F. & Richards, P.G., 1976. Comments on 'Damping of core waves' by A. Qamar and A. Eisenberg, *J. Geophys. Res.,* **81,** 3066–3068.

Cummins, P. & Johnson, L.R., 1988. Short-period body wave constraints of properties of the Earth's inner core boundary, *J. geophys. Res.,* **93,** 9058–9074.

Dziewonski, A.M. & Anderson, D.L., 1981. Preliminary reference earth model, *Phys. Earth planet. Inter.,* **25,** 297–356.

Dziewonski, A.M. & Gilbert, F., 1971. Solidity of the inner core of the Earth inferred from normal mode observations, *Nature,* **234,** 465–466.

Dziewonski, A.M. & Gilbert, F., 1976. The effect of small, aspherical perturbations on travel times and a re-examination of the corrections for ellipticity, *Geophys. J. R. astron. Soc.,* **44,** 7–17.

Engdahl, E.R., Flinn, E.A. & Romney, C.F., 1970. Seismic waves reflected from Earth's inner core, *Nature,* **228,** 852–853.

Engdahl, E.R., van der Hilst, R.D. & Buland, R.P., 1998. Global teleseismic earthquake relocation with improved travel times and procedures for depth determination, *Bull. seism. Soc. Am.,* **88,** 722–743.

Gilbert, F. & Dziewonski, A.M., 1975. An application of normal mode theory to the retrieval of structural parameters and source mechanisms from seismic spectra., *Phil. Trans. R. Soc. Lond.,* A, **278,** 187–269.

Gilbert, F., Dziewonski, A.M. & Brune, J.N., 1973. An informative solution to a seismological inverse problem, *Proc. Natl. Acad. Sci., USA,* **70,** 1410–1413.

Gubbins, D., 1977. Energetics of the Earth's core, *J. Geophys.,* **43,** 453–464.

Gubbins, D., Masters, T.G. & Jacobs, J.A., 1979. Thermal evolution of the Earth's core, *Geophys. J. R. Astron. Soc.,* **59,** 57–99.

Häge, H., 1983. Velocity constraints for the inner core inferred from long-period *PKP* amplitudes, *Phys. Earth planet. Inter.,* **31,** 171–185.

Hewitt, J.M., McKenzie, D.P. & Weiss, N.O., 1975. Dissipative heating in convective flows, *J. Fluid Mech.,* **68,** 721–738.

Kennett, B.L.N. & Engdahl, E.R., 1991. Traveltimes for global earthquake location and phase identification, *Geophys. J. Int.,* **105,** 429–465.

Kennett, B.L.N., Engdahl, E.R. & Buland, R., 1995. Constraints on seismic velocities in the Earth from traveltimes, *Geophys. J. Int.,* **122,** 108–124.

Loper, D.E., 1978. The gravitationally powered dynamo, *Geophys. J. R. Astron. Soc.,* **54,** 389–404.

Loper, D.E., 1991. The nature and consequences of thermal interactions twixt core and mantle, *J. Geomagn. Geoelectr.,* **43,** 79–91.

Masters, G., 1979. Observational constraints on the chemical and thermal structure of the Earth's deep interior, *Geophys. J. R. Astron. Soc.,* **57,** 507–534.

Masters, G. & Gubbins, D., 2003. On the resolution of density within the Earth, *Phys. Earth planet. Int.,* **140,** 159–167.

McElhinny, M.W. & Senanayake, W.E., 1980. Paleomagnetic evidence for the existence of the geomagnetic field 3.5 Ga ago, *J. geophys. Res.,* **85,** 3523–3528.

Schweitzer, J., 1992. PKiKP and PcP observations of the Chinese Nuclear Test on May 21, 1992 05:00 UTC, *EOS, Trans. Am. Geophys. Un.,* **73,** 408.

Shearer, P.M. & Masters, G., 1990. The density and shear velocity contrast at the inner core boundary, *Geophys. J. Int.,* **102,** 491–498.

Song, X. & Helmberger, D.V., 1995. A *P*-wave model of the Earth's core, *J. geophys. Res.,* **100,** 9817–1930.

Souriau, A. & Souriau, M., 1989. Ellipticity and density at the inner core boundary from sub-critical *PKiKP* and *PcP* data, *Geophys. J. Int.,* **98,** 39–54.

Stacey, F.D. & Stacey, C.H.B., 1999. Gravitational energy of core evolution: implications for thermal history and geodynamo power, *Phys. Earth planet. Int.,* **110,** 83–93.

Tkalčić, H., Romanowicz, B. & Houy, N., 2002. Constraints on *D*" structure using PKP(AB-DF), PKP(BC-DF) and PcP-P traveltime data from broadband records, *Geophys. J. Int.,* **148,** 599–616.